Articles

Redox Regulation of MAP Kinase Phosphatase 3†

Divya Seth and Johannes Rudolph*

Departments of Biochemistry and Chemistry, Duke University Medical Center, Durham, North Carolina 27710

Received January 24, 2006; Revised Manuscript Received April 26, 2006

ABSTRACT: MAP kinase phosphatase 3 (MKP3) is a protein tyrosine phosphatase (PTP) for which in vivo evidence suggests that regulation can occur by oxidation and/or reduction of the active site cysteine. Using kinetics and mass spectrometry, we have probed the biochemical details of oxidation of the active site cysteine in MKP3, with particular focus on the mechanism of protection from irreversible inactivation to the sulfinic or sulfonic acid species. Like other PTPs, MKP3 was found to be rapidly and reversibly inactivated by mild treatment with hydrogen peroxide. We demonstrate that unlike the case for some PTPs, the sulfenic acid of the active site cysteine in MKP3 is not stabilized in the active site but instead is rapidly trapped in a re-reducible form. Unlike the case for other PTPs, the sulfenic acid in MKP3 does not form a sulfenyl−amide species with its neighboring residue or a disulfide with a single proximate cysteine. Instead, multiple cysteines distributed in both the N-terminal substrate-binding domain (Cys147 in particular) and the C-terminal catalytic domain (Cys218) are capable of rapidly and efficiently trapping the sulfenic acid as a disulfide. Our results extend the diversity of mechanisms utilized by PTPs to prevent irreversible oxidation of their active sites and expand the role of the N-terminal substrate recognition domain in MKP3 to include redox regulation.

Reactive oxygen species (ROS)[1] are integral components of various signal transduction pathways (reviewed in ref *1*). For example, reversible oxidation and inactivation is a mechanism of regulation for the protein tyrosine phosphatases (PTPs) (*2*), regulators of many signal transduction pathways and of cell cycle control (*3*). Mitogen-activated protein kinase phosphatase 3 (MKP3), a member of the subfamily of PTPs known as dual-specificity phosphatases, has recently been added to this list of phosphatases regulated by oxidation. First, in human diploid fibroblasts, a correlation exists between the intracellular increase in the level of ROS and the decrease in the specific activity of MKP3 in senescent cells as compared to young cells (*4*). Second, ROS produced during downstream events following stimulation of cells by tumor necrosis factor α (TNFα) were shown to cause oxidative inactivation of MKP3 and consequential sustained activation of Jun N-terminal kinase (JNK) (*5*). ROS-mediated regulation of JNK-inactivating phosphatases therefore plays an important role in promoting the cell death processes of necrosis and apoptosis triggered by TNFα.

All PTPs, including MKP3, contain conserved sequence and structural features that allow them to be reversibly regulated by ROS. Although members of the PTP family differ sequentially and topologically, the active site motif (H/V)C(X)$_5$R(S/T) containing the catalytic cysteine is the defining characteristic of the PTPs. The pK_as of these catalytic cysteines are perturbed to 4.7−6.6 as compared to a typical value of 8.5 for a cysteine residue (*6*, *7*). The low pK_a of the active site cysteine makes it negatively charged at physiological pH, well suited for its role as a nucleophile in the formation of the thiol−phosphate intermediate, yet also highly susceptible to oxidation by ROS such as hydrogen peroxide (H_2O_2). Oxidation of the active site cysteine generates the sulfenic acid (Cys-SOH) and inactivates phosphatase activity. The Cys-SOH modification of PTPs can be readily reversed by numerous cellular reductants and can therefore be converted back to the thiolate to yield an active enzyme. Whereas in some cases it has been proposed that the sulfenic acid is the inhibited and reversible species (*5*, *8*), Cys-SOH is actually highly reactive and susceptible to rapid further oxidation to the sulfinic (Cys-SO_2H) or sulfonic acid (Cys-SO_3H). With the exception of the peroxiredoxins for which specific protein reductants exist (*9*), these higher oxidation states cannot be reduced to the active thiolate by typical biological reductants.

As in other dynamic regulatory mechanisms in signal transduction, it is crucial that the redox regulation of PTPs should be readily reversible. Different PTPs are now known

† This work was funded by NIH Grant R01 GM61822.

* To whom correspondence should be addressed. Phone: (919) 668-6188. Fax: (919) 613-8642. E-mail: rudolph@biochem.duke.edu.

[1] Abbreviations: ROS, reactive oxygen species; PTP, protein tyrosine phosphatase; MKP3, mitogen-activated protein kinase phosphatase 3; ΔMKP3, catalytic domain of MKP3; ΔC218S, C218S mutant of ΔMKP3; DTT, dithiothreitol; DTNB, 5,5′-dithiobis(2-nitrobenzoic acid); GSH, glutathione; TR, thioredoxin; TRR, thioredoxin reductase; 4-MUP, 4-methylumbelliferyl phosphate; mFP, *O*-methylfluorescein phosphate; IAA, iodoacetic acid; PTP1B, protein tyrosine phosphatase 1B; VHR, *Vaccinia* H1-related phosphatase; KAP, kinase-associated phosphatase; PTEN, phosphatase and tensin homologue; MALDI-MS, matrix-assisted laser desorption ionization mass spectrometry; ESI-MS, electrospray ionization mass spectrometry.

10.1021/bi060157p CCC: $33.50
Published on Web 06/27/2006

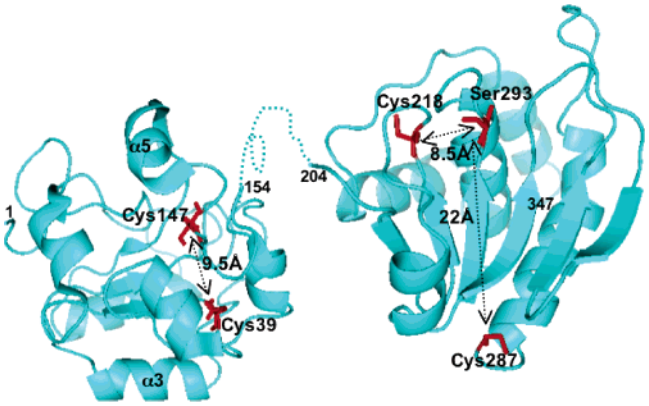

FIGURE 1: Structures of the N-terminal domain (1HZM) and C293S mutant of the C-terminal domain (1MKP) of MKP3 with the important cysteine residues highlighted in red. The two domains are connected by a dotted line. Approximate distances between the important cysteine residues have been indicated. Helices α3 and α5 in the N-terminal domain have been marked.

to employ different strategies to prevent the formation of irreversible oxidation states. Most commonly, the sulfenic acid serves as an intermediate to the formation of an intramolecular disulfide bond with a nearby cysteine. Stable disulfides between active site cysteines and these "backdoor" cysteines upon oxidation have been described in diverse phosphatases such as low-molecular mass PTP (LMW-PTP) (*10*), Cdc25 (*11*, *12*), phosphatase and tensin homologue (PTEN) (*13*), and kinase-associated phosphatase (KAP) (*14*). Alternatively, intermolecular disulfide bond formation has been described in receptor PTP (*15*). Besides the formation of disulfide bonds upon oxidation, a novel sulfenyl−amide species was formed between a main chain amide nitrogen and the sulfur of the active site cysteine in reversibly oxidized crystals of PTP1B (*16*, *17*).

The sequence and structural features that make PTPs susceptible to oxidation are also conserved in MKP3. The 381-amino acid protein contains an N-terminal substrate recognition domain and a C-terminal catalytic domain. Structural information for each separate domain is known, although their relative orientation with respect to each other is unknown (*18*, *19*) (Figure 1). The truncated C-terminal domain containing the active site cysteine (Cys293) retains enzymatic activity with artificial substrates (*20*). The N-terminal domain of MKP3 specifically interacts with the substrate ERK2, thus activating the catalytic domain for reaction with protein substrates (*21*−*23*). Interestingly, this N-terminal domain in MKP3s has two conserved regions of 10−15 amino acids known as Cdc25 homology domains (CH2-A and CH2-B). These regions are found in the catalytic domains of the Cdc25 phosphatases, a structurally unrelated class of dual-specificity phosphatases (*24*). In Cdc25s, the cysteine residue within the DCR sequence of the CH2-A domain is the backdoor cysteine that forms a disulfide bond with the active site cysteine upon oxidation (*11*, *25*). The conservation of this CH2-A motif between MKP3s and Cdc25s suggests the possible involvement of the N-terminal domain in the oxidative regulation of MKP3s.

Considering the in vivo significance of oxidative regulation of MKP3 recently reported (*5*), it is important to better understand the biochemical mechanism of MKP3 oxidation. We report here that MKP3, like other PTPs, is highly susceptible to oxidation by hydrogen peroxide. Also, we find that unlike the case for other PTPs, the involvement of multiple cysteine residues and one or more disulfide switches provides a mechanism for protecting the cysteine and bringing the disulfide to the surface of the protein, thus making it accessible for re-reduction by thioredoxin.

MATERIALS AND METHODS

Materials. 4-MUP was obtained from Molecular Probes. Thioredoxin/thioredoxin reductase (TR/TRR) from *Escherichia coli* was a generous gift from J. Stubbe (Massachusetts Institute of Technology, Cambridge, MA). Hydrogen peroxide (H_2O_2) was obtained from EM Science, and 100 mM stock solutions were prepared daily. Sequencing-grade trypsin was purchased from Promega. DTT, IAA, DTNB, catalase, NADPH, and mFP were purchased from Sigma.

Purification of MKP3 and MKP3 Mutants. The expression plasmid for MKP3 was a gift from J. Denu (University of Wisconsin, Madison, WI). It has the MKP3 coding sequence along with a carboxyl-terminal hexahistidine tag cloned as an NdeI−EcoRI fragment in the pT7-7 vector. The protein was purified as described previously (*20*) and was stored in aliquots at −80 °C in TNE buffer [50 mM Tris (pH 8.0), 50 mM NaCl, and 1 mM EDTA] with 2 mM DTT and 20% glycerol. Various mutants were generated using Quickchange mutagenesis (Stratagene) and the following primers: C218S, CCTGGGCTCTGCCAAGGACTC and CTTGGCAGAGCCCAGGTAAAGG; C287S, GGCAAAAACTCTGGTGTCCTGG and GACACCAGAGTTTTTGCCTCG; L294P, GTACATTGCCCGGCTGGCATTAGC and GCTAATGCCAGCCGGGCAATGTAC; C39S, CTGATGGACTCTCGACCGCAGG and CTGCGGTCGAGAGTCCATCAGC; C127S, GAGGGCTCTCGGGCGTTCTACC and GTAGAACGCCCGAGAGCCCTCG; and C147S, GCCCTGCACTCTGAGACC and GGTCTCAGAGTGCAGGGCG. The catalytic domain constructs (ΔMKP3 and ΔC218S) were generated by PCR from the appropriate full-length MKP3 using the following primers: GATTCGCATATGCCTTCCTTCCCG and CGAATCGAATTCAGTGATGGTGATGGTGATGCAGGGTCCTTTC. The PCR products including a carboxyl-terminal hexahistidine tag were cloned in the pT7-7 vector as NdeI−EcoRI fragments. The mutant and catalytic domain proteins were purified as described for the wild type.

Rate of Inactivation by H_2O_2. The rate of inactivation of MKP3 was calculated using a fixed time-point quench protocol. MKP3 (7 μM) was incubated with varying concentrations of H_2O_2 (from 0.25 to 1.0 mM) in TNE buffer at 20 °C. At varying time points (from 30 s to 10 min), an aliquot was taken and diluted (20-fold) into TNE buffer containing 14 units of catalase. Phosphatase activities were measured immediately with 1 mM 4-MUP by using a continuous assay that monitors product formation by fluorescence with excitation at 390 nm and emission at 460 nm in a Polarstar plate reader. The percent remaining activities were determined by comparison with mock-treated samples. The observed rate constant of inactivation (k_{obs}) was determined by fitting the data to eq 1.

$$\text{percent remaining activity} = 100e^{-k_{obs}t} + \text{remaining activity} \quad (1)$$

Scheme 1: Possible Reaction Pathways for Oxidation and/or Reduction of the Active Site Cys293 of MKP3[a]

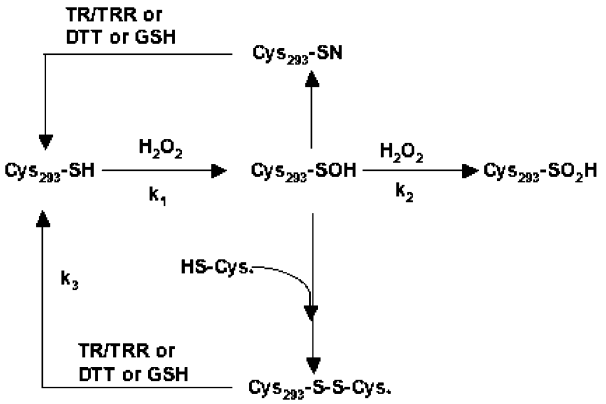

[a] Following oxidation of Cys293 to the sulfenic acid (−SOH), further oxidation could lead to the sulfinic acid ($-SO_2H$). Alternatively, the sulfenic acid can be trapped by either a sulfenyl−amide species (−SN) or a disulfide with an unidentified backdoor cysteine that has been denoted with an asterisk. Re-reduction of the sulfenyl−amide species or the disulfide leads to reactivation of MKP3.

The second-order rate constant, k_1 (Scheme 1), was obtained by fitting the linear dependence of the rate of inactivation (k_{obs}) on the concentration of H_2O_2.

Reactivation of MKP3. To determine the reactivation rates, MKP3 (3.5−10 μM) was incubated with 1 mM H_2O_2 for 10 min to inactivate the enzyme. Aliquots were then diluted 2-fold into TNE buffer containing 14 units of catalase and varying amounts of DTT (2.5−40 mM). Following incubation under reducing conditions for varying amounts of time (2.5−30 min), aliquots were diluted 20-fold and the phosphatase activity was measured by adding 1 mM 4-MUP and monitoring product formation. Reactivation rates with TR/TRR were determined using mFP (100 μM, $\epsilon_{477} = 27\,000$ M^{-1} cm^{-1}) as the substrate instead of 4-MUP to avoid interference from NADPH in fluorescence reading at 460 nm. These reactivation reactions were performed in the absence of DTT using TR (0.25−4 equiv) and NADPH (60−960 μM), with a ratio of TR to TRR of 250:1. The observed rate constant of reactivation (k_{react}) was determined by fitting the data to eq 2.

$$\text{percent recovered activity} = 100(1 - e^{-k_{react}t}) + \text{remaining activity} \quad (2)$$

The second-order rate constant, k_3 (Scheme 1), was obtained by fitting the linear dependence of the rate of reactivation on the concentration of the reductant. Control experiments confirmed that the rates of reactivation were independent of the concentration of TRR and NADPH.

Reversibility of Inactivation. The reversibility of inactivation of ΔC218S was determined by using a partitioning experiment as detailed in ref *12*. Briefly, the inactivation reaction was carried out as described above with an additional incubation with or without 50 mM DTT in the catalase-containing quench solution. The relative amounts of reversibly inactivated MKP3 (sulfenic acid and/or intramolecular disulfide forms) and irreversibly inactivated MKP3 (sulfinic and/or sulfonic acids) were determined by comparing the activity using 4-MUP. The observed rate of accumulation of unrecoverable activity (k_{obs}) was determined by fitting the data to eq 3.

$$\text{percent unrecoverable activity} = 100(1 - e^{-k_{obs}t}) + \text{remaining activity} \quad (3)$$

The remaining activity determined in a separate control arises from incomplete oxidation in the inactivation reaction and is typically 1−5% of the full activity. Numerical integration of eqs 4 and 5 was used to model the overall time course of the reaction.

$$\delta[SOH]/\delta t = k_1[H_2O_2][SH] - k_2[H_2O_2][SOH] \quad (4)$$

$$\delta[SO_2H]/\delta t = k_2[H_2O_2][SOH] \quad (5)$$

where k_1 and k_2 reflect the first and second oxidation, respectively, of the active site cysteine (Scheme 1). The numerical integration was separated into parts in various columns of an Excel worksheet where the exact differential, δt, was replaced with the interval Δt. A Δt of 2 s was sufficiently small to accurately represent a continuous process.

Thiol Titration. Titration of free thiols in MKP3 was performed using Ellman's reagent (DTNB). Typically, 100−250 μM MKP3 was treated with 1−3 mM H_2O_2 for 10 min (oxidized sample) or 50 mM DTT for 30 min (reduced sample) in a volume of 50 μL. The protein was separated from small molecules by gel filtration on G-50 Sephadex (0.3 cm × 20 cm) in 100 mM Tris (pH 8.0). The free thiols in the protein sample were determined at 412 nm following incubation with varying amounts of MKP3 (0.3−2 μM) and 500 μM DTNB ($\epsilon = 13\,600$ M^{-1} cm^{-1}). Reversible inactivation in the oxidized sample was tested by measuring the activity before and after reactivation with 50 mM DTT for 30 min. Protein concentrations were determined using the Bio-Rad reagent.

Mass Spectrometry. Samples for matrix-assisted laser desorption mass spectrometry (MALDI-MS) were prepared by trypsin digestion of 10−50 μg of protein with or without H_2O_2 treatment. If free cysteines were blocked with IAA prior to digestion, the protein sample was next treated with IAA (100 mM) for 30 min. Next the reaction mixture was diluted more than 10-fold in TNE buffer in an Amicon concentrator (Millipore) with a 10 kDa molecular mass limit and centrifuged to rapidly separate the protein from excess H_2O_2 and/or IAA. Ammonium bicarbonate (100 mM, pH 7.8) was added to the protein to obtain a final concentration of 50 mM. The protein was digested with 1 μg of sequencing-grade trypsin by overnight incubation at 37 °C. The digestion mix was desalted with a C_{18}-ZipTip (Millipore). The peptides were then analyzed by MALDI-TOF using the Voyager DE-Pro instrument from Applied Biosystems. For separation of tryptic peptides prior to MALDI analysis, we used a reverse-phase high-performance liquid chromatography (HPLC) system comprised of a Varian Prostar 210 solvent delivery module, a Varian Prostar 320 UV−vis detector operating at 220 nm, and a Jupiter Proteo 90 Å, 4 μm, C12 (250 mm × 4.6 mm) (Phenomenex) column. Elutions were performed using a 0 to 60% gradient consisting of 0.1% (v/v) TFA (solution A) and acetonitrile containing 0.1% (v/v) TFA (solution B) at a flow rate of 1 mL/min, and fractions (300 μL) were collected. The fractions were concentrated 10-fold

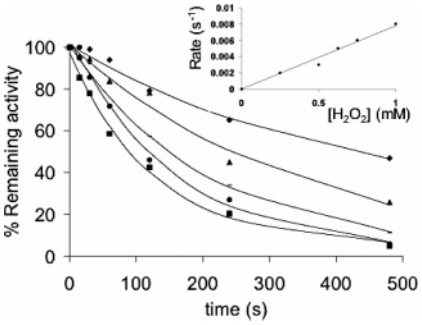

FIGURE 2: Time dependence of inactivation of MKP3 by H_2O_2. The reactions were performed as described in Materials and Methods, and the curves were obtained by fitting the data to eq 1. The following concentrations of H_2O_2 were used: 250 μM (◆), 500 μM (▲), 625 μM (−), 750 μM (●), and 1 mM (■). In the inset, the concentration dependence of the rate of inactivation was used to derive a second-order rate constant, k_1, of 9.6 ± 1.1 M^{-1} s^{-1} (Scheme 1). Data are representative of at least three independent determinations.

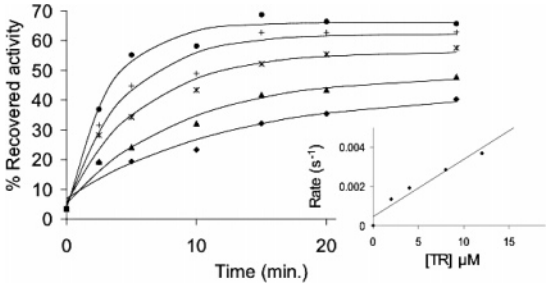

FIGURE 3: Time dependence of MKP3 reactivation by thioredoxin. The reactions were performed as described in Materials and Methods, and the curves were obtained by fitting the data to eq 2. The following concentrations of thioredoxin were used: 2 (◆), 4 (▲), 8 (∗), 12 (+), and 16 μM (●). In the inset, the concentration dependence of the rate of reactivation was used to derive a second-order rate constant, k_3, of 316 ± 17 M^{-1} s^{-1} (Scheme 1). Data are representative of at least two independent determinations.

using a Speed-Vac and analyzed by MALDI-TOF. Collisional dissociation tandem mass spectrometry (MS/MS) was performed using a QSTAR XL quadrupole time-of-flight tandem mass spectrometer (ABI/MDS-Sciex) equipped with an electrospray source. MS data acquisition and analysis were performed using Analyst QS.

RESULTS

Rapid Inactivation of MKP3 by H_2O_2 and Reactivation by DTT and TR/TRR. Strong evidence has already shown a physiological role for regulation of MKP3 by oxidation (*4*, *5*); thus, its reactivity inside the cell has been established. However, determining the relative reactivity of MKP3 in comparison to other PTPs known to be susceptible to oxidation is of interest as well as its relative reactivation by the cellular reductants thioredoxin and glutathione. To determine the reactivity of MKP3 toward oxidation, the enzyme was incubated with varying concentrations of H_2O_2 for varying amounts of time. The reactions were quenched by dilution into a buffer containing catalase, and the residual phosphatase activity was measured using 4-MUP (Figure 2). Control experiments showed that catalase was sufficient to deplete the H_2O_2 (data not shown). The rate of inactivation of MKP3 at 20 °C and pH 8.0 varied linearly as a function of H_2O_2 concentration with a second-order rate constant of 9.6 ± 1.1 M^{-1} s^{-1}. This is comparable to the rates of inactivation of PTP1B and VHR of 9.1 and 17.9 M^{-1} s^{-1}, respectively (*8*), and is ∼15- fold slower than the rate of inactivation of Cdc25B (*12*). The inactivation rate of MKP3 is 10-fold higher than the reaction rates for glutathione (0.87 M^{-1} s^{-1}, 37 °C, pH 7.4) (*26*) and thioredoxin (1.05 M^{-1} s^{-1}, 25 °C, pH 7.4) (*27*) with H_2O_2, which is apparently sufficient to allow for oxidation in vivo.

Having established suitable conditions for oxidative inactivation of MKP3, we next determined the reversibility of oxidation by reductants such as DTT and thioredoxin. The rate of reactivation of MKP3 was measured by first inactivating the protein with 1 mM H_2O_2 for 10 min and then quenching into a buffer containing catalase and varying amounts of reducing agents. After further incubation to allow re-reduction of the catalytic cysteine, the recovery of activity was measured as a function of time (Figure 3). The rate of reactivation varied linearly as a function of reductant concentration, and the second-order rate constant with TR/TRR was 316 ± 17 M^{-1} s^{-1}. The rate of reactivation of MKP3 with TR/TRR was 3-fold lower than that of Cdc25B (*12*) and suggests that differences in the rates of inactivation and reactivation of various PTPs may add an additional level of fine-tuning for intracellular redox regulation. Using glutathione or DTT, the second-order rate constant was only 1−2 M^{-1} s^{-1} (data not shown). Although DTT was slower at reducing MKP3 than TR/TRR, 50 mM DTT could completely reactivate oxidized MKP3 in 30 min and was thus used to determine the reversibility of inactivation of MKP3 and its various mutants by oxidation for most subsequent experiments.

Finding that MKP3 is indeed readily susceptible to reversible inactivation by oxidation/reduction led us to next probe the molecular mechanism of this process. Given the precedence from other PTPs of oxidation at active site cysteines, we assumed Cys293 in MKP3 was the primary target of H_2O_2, as supported by subsequent MALDI-MS data (see below). Thus, our approach was focused on the more interesting and open question, namely, how the active site Cys293 is protected from irreversible inactivation to higher oxidation states.

Identification of the Backdoor Cysteine Residue in the Catalytic Domain. In all PTPs currently known to form an intramolecular disulfide upon oxidation, the backdoor cysteine is always present within the catalytic domain, within 10 Å of the active site cysteine in the unoxidized protein (*10*, *11*, *14*, *28*, *29*). MKP3 contains nine cysteines in addition to Cys293 of the active site. The relative location with respect to the active site of six of these (Cys39, Cys80, Cys90, Cys127, Cys147, and Cys155) in the N-terminal substrate recognition domain is not known (Figure 1). Of the three remaining cysteines in the C-terminal domain of MKP3, Cys218 was identified as the most likely backdoor cysteine residue, with a sulfur−sulfur distance of 8.5 Å (Figure 1). Cys287, although within the same tryptic peptide as Cys293, is 22 Å distant through space. To simplify the analysis of Cys218 as a potential backdoor cysteine, we chose first to study the catalytic domain alone, consisting of residues 204−347. This region encompasses the stable domain used for determining the X-ray structure of the catalytic domain of MKP3 and has phosphatase activity with pNPP and ERK2 (*18*). If Cys218 is the backdoor cysteine, we expect its

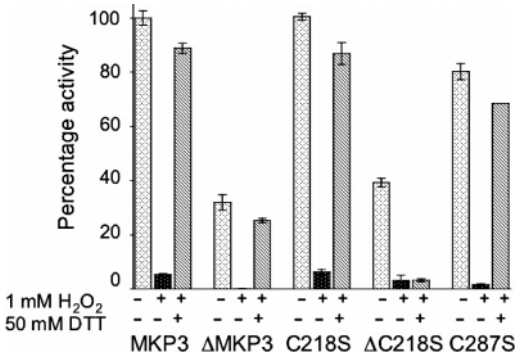

FIGURE 4: Bar graph showing catalytic activities of MKP3, ΔMKP3, C218S, and ΔC218S. The proteins (7 μM) were treated with 1 mM H_2O_2 for 10 min for oxidation and with 50 mM DTT for 30 min for re-reduction. The activities were measured with 4-MUP and are expressed as a percentage of the starting activity of MKP3. Averages and standard deviations from at least two independent experiments are shown.

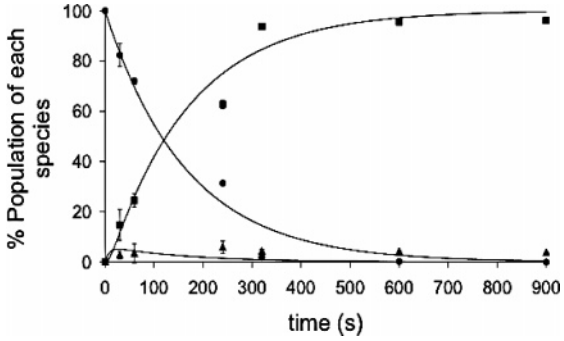

FIGURE 5: Time course for depletion of free thiolate (●), formation of sulfenic acid (▲), and accumulation of higher oxidation states (■). The data and simulated curves were generated as described in Materials and Methods using a k_1 of 6 M^{-1} s^{-1} and a k_2 of 101 M^{-1} s^{-1}. Averages and standard deviations from at least two independent experiments are shown.

mutation to cause irreversible inactivation of MKP3 by oxidation with H_2O_2. As expected, the catalytic domain of MKP3 (ΔMKP3) and its potential backdoor mutant, ΔC218S, retained good phosphatase activity toward 4-MUP (within 3-fold of that of MKP3, Figure 4). Also, like full-length MKP3, ΔMKP3 could be readily inactivated by oxidation with H_2O_2 and re-reduced to yield essentially full activity with DTT (Figure 4). However, the inactivation of ΔC218S with H_2O_2 treatment was irreversible, as activity was not recovered upon incubation with DTT (Figure 4).

The efficiency of Cys218 as a trap of the sulfenic acid is demonstrated by the consistently high recovery of activity of ΔMKP3 upon reduction with DTT. To investigate this efficiency more quantitatively, a partitioning experiment was performed. ΔC218S was incubated with 1 mM H_2O_2, and at varying times, aliquots were diluted into a buffer containing either only catalase or catalase and DTT. Further incubation allowed for reactivation of the sulfenic acid intermediate, whereas the terminal sulfinic acid species cannot be reactivated. Therefore, the ratio of phosphatase activities determined using 4-MUP reveals the relative pools of sulfenic and sulfinic species after oxidation. The data for the free thiolate, sulfenic, and sulfinic forms were fitted to curves generated by numerical integration of eqs 3 and 4 (Figure 5) and indicate a buildup of <5% of the sulfenic acid intermediate during oxidation of ΔC218S. Thus, once the sulfenic acid is formed from the thiolate ($k_1 = 6$ M^{-1} s^{-1}, in agreement with data in Figure 2), the second oxidation step to sulfinic acid ($k_2 = 101$ M^{-1} s^{-1}) is a rapid process in the ΔC218S mutant. In conjunction with the high recovery of activity after re-reduction, this result emphasizes the efficiency of trapping by the backdoor Cys218 in ΔMKP3. Also, the instability of the sulfenic acid is consistent with the fact that the sulfenic acid is not detected by MALDI-MS following oxidation of MKP3 (see Figure 6 below).

Cys218 Is Not the Sole Backdoor Cysteine in Full-Length MKP3. Having identified Cys218 as the backdoor cysteine in the context of the catalytic domain ΔMKP3, we next investigated its role in the full-length protein. The C218S mutant of full-length MKP3 has phosphatase activity comparable to that of the wild-type protein and, like the wild type, was completely inactivated upon incubation with 1 mM H_2O_2 for 10 min (Figure 4). In contrast to that of ΔC218S, the activity of C218S inactivated by oxidation could essentially be completely recovered following reduction with DTT (Figure 4). Thus, in the intact MKP3 protein, the reversibility of inactivation does not rely on Cys218. The mechanism for protecting the active site cysteine from excessive oxidation in full-length MKP3 is still highly efficient, but clearly more complex than the case for the catalytic domain by itself. Given the high reactivity of the sulfenic acid toward further oxidation (Figure 5), this alternative mechanism must also be highly efficient and may represent a physiologically relevant mechanism of protection.

MS Analysis of the Tryptic Peptide Containing Cys293. We used mass spectrometry to further investigate the mechanism by which the active site cysteine in MKP3 is protected from excess oxidation. For simplicity, we again focus first on the catalytic domain (ΔMKP3) and the ΔC218S mutant, in both their reduced and oxidized forms. In untreated ΔMKP3 and ΔC218S, the tryptic peptides containing Cys293 ($NC_{287}GVLVHC_{293}LAGISR$) have a mass of 1442 Da (Figure 6). Given the irreversible oxidation seen for the ΔC218S mutant following oxidation (Figure 4), we expected to identify a tryptic dipeptide comprised of the disulfide-linked peptides containing Cys218 and Cys293 (5012 Da) for oxidized ΔMKP3 and a sulfinic acid-modified peptide for oxidized ΔC218S (1474 Da). This expectation did hold true for the ΔC218S mutant, which revealed the presence of a novel tryptic peptide with a molecular mass of ~1475 Da corresponding to the formation of sulfinic acid at the catalytic cysteine (Figure 6). For the oxidized wild-type catalytic domain, however, we instead observed that the same peptide had a mass of 1440 Da (Figure 6). This mass difference compared to the reduced protein was also observed for full-length MKP3, where the experiment was repeated four times to confirm the difference of 2 Da (1442.36 ± 0.15 Da for reduced MKP3 vs 1440.33 ± 0.13 Da for oxidized MKP3) (Figure 6). The two forms of the peptide also had reproducibly different times of elution from the HPLC column (53 vs 51% acetonitrile), as is evident by the presence of different coeluting peptides (Figure 6). The reproducible mass difference and the altered mobility by HPLC are consistent with the formation of an intrapeptide disulfide between Cys287 and the active site Cys293.

To confirm the assignment of the MS peak to the intrapeptide disulfide from oxidized ΔMKP3 and MKP3, we

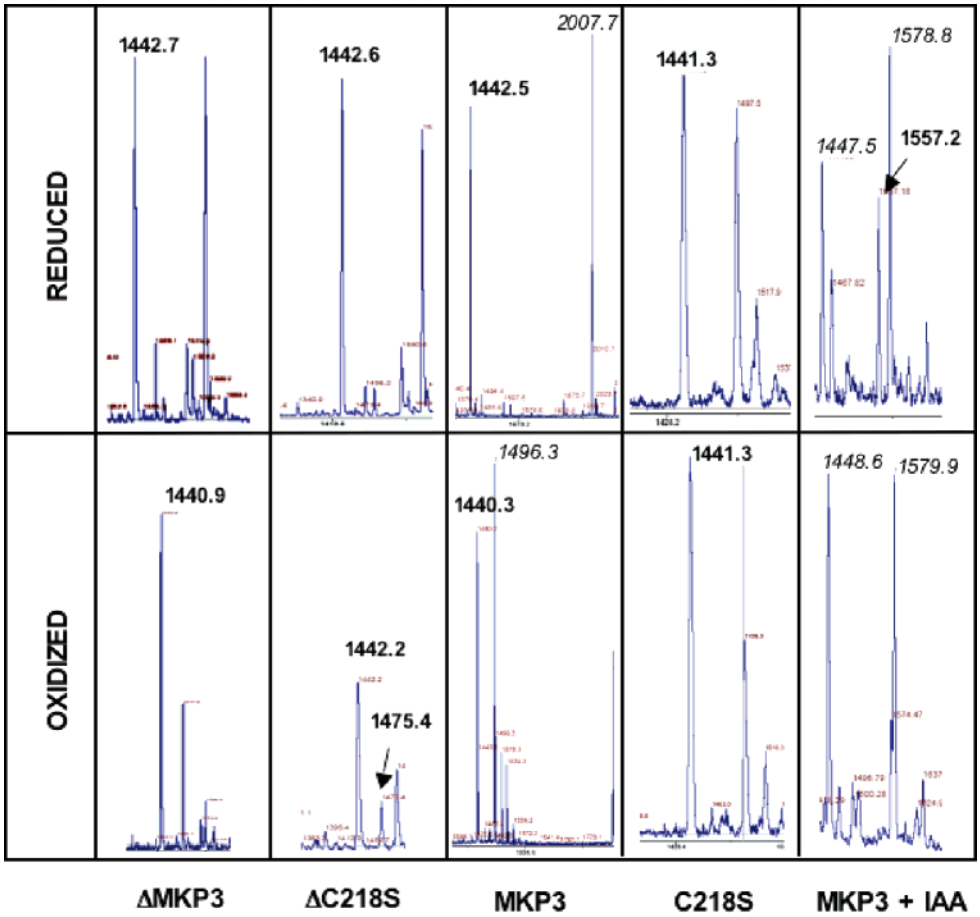

FIGURE 6: MALDI-MS mass spectra of reduced and oxidized MKP3. The region of the MALDI-MS spectrum containing the active site tryptic peptide $NC_{287}GVLVHC_{293}LAGISR$ is shown for ΔMKP3, ΔC218S, MKP3, C218S, and MKP3 treated with IAA, from left to right, respectively. The data for samples from reduced (50 mM DTT, 30 min) and oxidized protein (1 mM H_2O_2, 10 min) are shown in the top and bottom rows, respectively. The active site peptide is labeled in bold type, and other significant peptides are labeled in italic type. The oxidized samples of MKP3 and ΔMKP3 show a loss of 2 Da compared to reduced protein, consistent with formation of an intrapeptide disulfide. The C218S mutant shows no change in mass upon oxidation. The oxidized sample of ΔC218S shows the presence of a peptide corresponding to the formation of sulfinic acid with the addition of two oxygen molecules to the peptide containing Cys293. The remaining unoxidized peptide seen in the sample for ΔC218S probably arises from a fraction of the enzyme existing in an inactive state wherein the active site cysteine is not a thiolate that is highly susceptible to oxidation under mild treatment with hydrogen peroxide. IAA-treated MKP3 shows a doubly carboxymethylated active site peak in the reduced sample, with the disappearance of the active site peptide in the oxidized sample. Reference peaks in this sample have been shown for comparison to indicate that the samples were processed correctly.

turned to collisional dissociation tandem mass spectrometry (MS/MS) analysis of the tryptic peptide with fragmentation at each residue. Fragmentation of the reduced peptide gave peaks corresponding to the expected b-ions (fragmentation from the N-terminus) and y-ions (fragmentation from the C-terminus) (Table 1). However, the peaks corresponding to y_7 and y_8 ions from the oxidized peptide showed an increase of 32 Da that was due to the addition of a sulfur atom to this fragment. The two new fragments are formed due to the cleavage of the C−S bond of Cys287, followed by fragmentation of the backbone N-terminal to residues Cys293 and His292, respectively. This result confirms the presence of an intrapeptide disulfide bond between the two cysteine residues within the peptide and explains the observed decrease in mass of 2 Da of the active site peptide upon oxidation of ΔMKP3 and MKP3.

In the intact protein, the distance between the two cysteine residues found as a disulfide in MS analysis of this peptide is 22 Å (Figure 1). Because the average length of a disulfide bond in proteins is ~2.1 Å, direct disulfide bond formation between Cys287 and Cys293 is not possible without a massive conformational change following oxidation. Although disulfide formation upon oxidation has been shown to significantly alter the conformation of the active site loop in Cdc25B (*25*), the much larger conformational change required to produce a disulfide bond between Cys293 and Cys287 in MKP3 seems highly unlikely given the core location of the α-helix in which both these residues are found. We hypothesized instead that Cys293 first forms a disulfide with the Cys218 residue we identified above as the backdoor cysteine. This initial Cys293−Cys218 cystine, by disulfide exchange during the reaction workup, subsequently leads to the formation of the entropically favored intrapeptide disulfide bond (Cys293−Cys287). In agreement with this interpretation, the C287S mutant retains full activity and can be reversibly inactivated by treatment with H_2O_2 and DTT (Figure 4).

We next performed MALDI-MS analysis of tryptic fragments of the full-length backdoor C218S mutant to analyze the results of oxidation. As for the catalytic domain, the reduced sample of C218S shows the intact active site peptide, as expected (~1442 Da) (Figure 6). Following oxidation,

Table 1: Ions Observed upon Fragmentation of the Active Site-Containing Peptide[a]

expected fragment (Da)	observed in the reduced peptide (Da)	observed in the oxidized peptide (Da)
b_2, 218.06	218.06	ND[b]
b_3, 275.08	275.08	ND[b]
b_4, 374.15	374.15	ND[b]
b_5, 487.23	487.23	ND[b]
y_1, 175.11	ND[b]	175.11
y_2, 262.12	ND[b]	262.15
y_4, 432.26	ND[b]	432.25
y_5, 503.29	ND[b]	503.28
y_6, 616.38	ND[b]	616.37
y_7, 719.39	ND[b]	**751.35**
y_8, 856.45	856.44	**888.38**
y_9, 955.51	955.51	ND[b]
y_{10}, 1068.60	1068.58	ND[b]

[a] Masses of fragments obtained from MS/MS of the reduced and oxidized active site-containing $NC_{287}GVLVHC_{293}LAGISR$ peptide. The expected masses are given for comparison. The y_7 and y_8 ions that differ from the expected are denoted in bold type and indicate an intrapeptide disulfide between Cys287 and Cys293. [b] Not detected.

the active site peptide from C218S is not seen with its mass reduced by 2 Da but instead retains the signal for the reduced active site peptide (1442 Da, not 1440 Da) (Figure 6). Higher oxidation states (sulfinic or sulfonic) were not observed for C218S. That is, when Cys218 is not present, the active site cysteine first forms a disulfide with a different cysteine, presumably in the N-terminus, leading to reversibly inactivated MKP3 (Figure 4). The free active site cysteine that is seen in the oxidized sample is regenerated, presumably again by disulfide exchange (e.g., involving Cys147 and Cys155; see below).

To block disulfide exchange during the workup and thus potentially identify novel intramolecular disulfides that would reveal the identity of potential alternative backdoor cysteines in the context of full-length MKP3, we turned to pretreatment with IAA prior to trypsin digestion. We observed the doubly carboxymethylated active site peptide in MALDI-MS (1558 Da) for the reduced but not oxidized protein (Figure 6). Similar results were seen for the C218S mutant (data not shown). This result is consistent with Cys293 and Cys287 being free thiols in the reduced protein and the active site cysteine forming a novel disulfide upon oxidation. However, no corresponding new higher-molecular mass peaks could be identified despite extensive efforts using MALDI- or ESI-MS, even following fractionation by HPLC. Unfortunately, this is a common problem for high-molecular mass peptides. Some of the tryptic peptides containing cysteine (including Cys218) range from 3300 to 5300 Da prior to disulfide formation with the active site peptide. Digestion with other proteases that should yield smaller fragments did not lead to consistent cleavage products.

Multiple Cysteines Serve To Protect the Active Site Cysteine in MKP3. Besides the three cysteine residues (Cys218, Cys287, and Cys293) already considered in this study, full-length MKP3 has seven other cysteines. All of these cysteines are accessible to DTNB titration and found as free cysteines in the reduced protein (9.8 ± 0.7 equiv). DTNB titration of oxidized MKP3 yields only 3.3 ± 0.7 equiv, indicating that three disulfides are formed in the oxidized protein and suggesting that multiple other cysteines are involved in protecting the active site cysteine. To confirm that oxidation of these multiple cysteines is dependent on initial oxidation at the active site, we performed the DTNB titration following oxidation in the presence of 200 mM inorganic phosphate. Analogous to the cases of PTP1B (*8*) and Cdc25B (*12*), phosphate should bind in the active site loop and protect Cys293 from oxidation. As expected, treatment with H_2O_2 in the presence of phosphate effectively protected the active site cysteine, with 74% remaining activity compared to <2% in the control without phosphate. The DTNB titration of this sample revealed 7.4 ± 1.2 remaining cysteines. Although the relative homogeneity or heterogeneity of oxidation and inactivation is not known, this result is consistent with the oxidation of multiple cysteines being dependent on oxidation occurring at the active site first. In fact, coupled with the observed regeneration of the reduced active site peptide in the oxidized sample of the C218S mutant (Figure 6), these results suggest that multiple remote disulfides yield inactive MKP3, even when the active site cysteine is not tied up in one of these disulfides.

Only two of the six possible N-terminal cysteines are completely conserved among known MKP3s, namely, Cys39 and Cys147 (Figure 1). These two cysteines lie within two previously described Cdc25 homology domains (*24*) for which no specific function has yet been assigned in the MKP3 family. Although these Cdc25 homology domains have no apparent structural homology between the MKP3s and the Cdc25s, it is intriguing to note that $DC_{39}R$ in MKP3 corresponds to $DC_{426}R$ in Cdc25B, wherein Cys426 is the backdoor cysteine for Cdc25B (*12*). Cys147 is part of the second Cdc25 homology domain, which in Cdc25B is Cys484. The nonconserved cysteines include Cys80, Cys90, Cys127, and Cys155 in the N-terminal domain and Cys353 in the catalytic domain.

Because of the complexity of multiple pathways involving numerous cysteines (see the Discussion), we focus here on the potential involvement of the two conserved cysteines, Cys39 and Cys147. As Cys218 can protect the catalytic cysteine from further oxidation in the catalytic domain and full-length MKP3, we generated individual mutations of these two potential backdoor mutants in the context of the C218S mutant. Both C39S/C218S and C147S/C218S had phosphatase activity toward 4-MUP comparable to that of the wild type (Figure 7). Also, like the wild type, both of these mutants could be inactivated with 1 mM H_2O_2, and subsequently reactivated with 50 mM DTT (Figure 7). The reversibility of oxidative inactivation for these mutants indicates that neither Cys39 nor Cys147 alone is the only N-terminal cysteine able to rapidly and effectively form a protective disulfide with the active site cysteine. These results are consistent with the DTNB titrations. Similar results were seen for C127S/C218S and C353S/C218S (data not shown). Other double-cysteine mutants or multiple simultaneous mutations of cysteines (e.g., C39S/C147S/C218S) yielded insoluble protein not amenable to assays and inactivation studies.

Cys147 Plays an Important Role in the Reduction of MKP3. We next tested the potential involvement of Cys39 and Cys147 in the reactivation of MKP3 by thioredoxin. Recall that thioredoxin reduces oxidized MKP3 ~150-fold more efficiently than DTT and is the likely cellular reductant. Reactivation of the catalytic domain ΔMKP3 with thio-

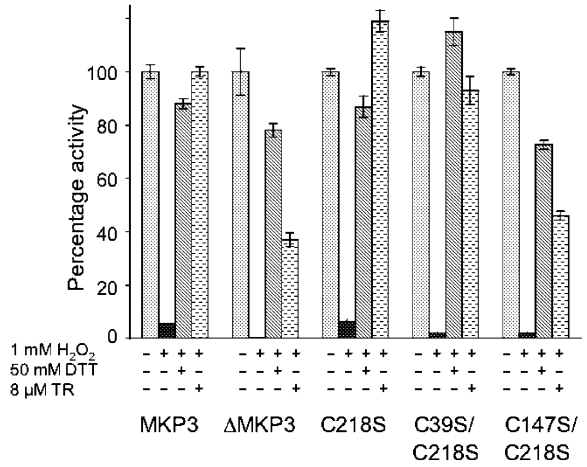

FIGURE 7: Bar graph showing catalytic activities of MKP3, C39S/C218S, C127S/C218S, C147S/C218S, and C353S/C218S. The proteins (7−10 μM) were treated with 1 mM H_2O_2 for 10 min for oxidation. For reactivation with 50 mM DTT, the proteins were treated for 30 min, and the activities were measured with 4-MUP and are expressed as a percentage of the activity of the untreated control. For reactivation with thioredoxin, the proteins were treated with 8 μM thioredoxin for 15 min (including 32 nM TRR and 480 μM NADPH), and activities were measured with mFP and are expressed as a percentage of the wild-type rate of reactivation for each protein assuming a first-order reactivation as seen in Figure 3. Averages and standard deviations from at least two independent experiments are shown.

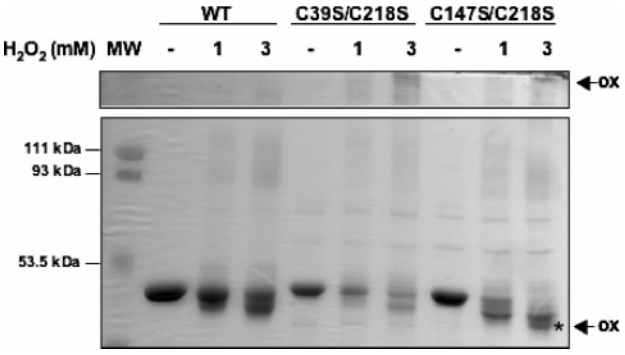

FIGURE 8: Nonreducing SDS−PAGE of MKP3. MKP3 and the C39S/C218S and C147S/C218S mutants were treated with increasing concentrations of H_2O_2, as indicated. The samples were subjected to SDS−PAGE under nonreducing conditions. An asterisk denotes the unique faster-migrating form of the C147S/C218S mutant. Higher-molecular mass aggregates were also detected for these two mutants, as bands near the loading well and by the apparent loss of staining intensity at the lower molecular masses. The C127S/C218S and C353S/C218S mutants behaved like wild-type MKP3 (not shown).

redoxin is not as efficient as for the wild type (Figure 7). In the context of the full-length protein, the C218S and C39S/C218S mutants were identical to the wild type whereas the C147S/C218S mutant behaved like ΔMKP3, namely, significantly slower at being re-reduced by thioredoxin (Figure 7). A similar result was seen for the C147S mutant alone (data not shown). This indicates a role particularly for Cys147 in the interaction and disulfide bond formation with thioredoxin. A special role for Cys147 compared to Cys39 is consistent with a unique faster-migrating form of oxidized C147S/C218S observed in a nonreducing gel-based assay, as if the absence of Cys147 leads to an alternative compact form of the protein (Figure 8).

MS Analysis of the Tryptic Peptide of MKP3 Containing Cys147. To provide further evidence for the involvement of Cys147 in the mechanism of protection from excessive oxidation, we again turned to MALDI-MS. Cys147 lies within a tryptic peptide with a molecular mass of 3404 Da that also contains Cys155. In reduced MKP3, this peptide is detected at 3404 Da and is found doubly carboxymethylated following treatment with IAA (3520 Da, Figure 9). In oxidized MKP3, this peptide appears to contain an intrapeptide disulfide with a molecular mass of 3402 Da, as seen for both the untreated and IAA-treated samples (Figure 9). As for the active site peptide, the thermodynamically more favored product is found, even after IAA trapping of free cysteines that prevents disulfide exchange during the workup. On the basis of the NMR structure of the N-terminal domain, this appears feasible, as Cys147 and Cys155 are quite close in three-dimensional space. Although Cys155 is not defined in the structure of the N-terminus of MKP3 (the last visible residue is Ser154; Figure 1), Cys147 lies near the end of a turn that would loop Cys155 into its proximity. In the C218S mutant, the same doubly carboxymethylated peptide is seen from the reduced and oxidized proteins (data not shown). Thus, the Cys147−Cys155 disulfide can form in a manner independent of Cys218. Because this intrapeptide disulfide is found even when disulfide exchange is blocked by IAA treatment during workup of the oxidized protein, the Cys147−Cys155 disulfide must be a primary and relevant product of oxidation.

To further confirm these molecular mass assignments and study the role of Cys147 in more detail, we performed MALDI-MS analysis of the C147S/C218S mutant before and after oxidation (Figure 9). As expected, the tryptic peptide from the reduced protein shows only one alkylation event. The tryptic peptide from oxidized MKP3 is also found singly alkylated. Our interpretation is that formation of a disulfide between Cys293 (or some other intermediary cysteine, but not Cys218) and Cys147, but not Cys155, is a primary mechanism by which MKP3 responds to oxidation. Thus, although multiple cysteines can trap the active site cysteine, some specificity exists, and it is not solely a matter of random collisions.

A Sulfenyl−Amide Species between Cys293 and Leu294 Is Not on the Reaction Path. Crystal structures of PTP1B have revealed formation of a sulfenyl−amide species upon oxidation (*16*, *17*). In PTP1B, the sulfur atom of the catalytic cysteine forms a bond with the backbone nitrogen of the adjacent residue (on the C-terminal side) to generate a five-membered ring. It was proposed that the reaction occurs by nucleophilic attack of the backbone nitrogen of Ser216 on the sulfur atom of the sulfenic acid at the active site cysteine, Cys215, and recent elegant model chemistry has supported this chemically unlikely reaction (*30*). In MKP3, the corresponding residues are the catalytic cysteine, Cys293, and the adjacent residue, Leu294. Although we believe that cysteines play the main protective role against excessive oxidation, it is nominally possible that a sulfenyl−amide species is an obligate intermediate on the reaction path. Such a sulfenyl−amide species, although in theory detectable by a loss of 2 Da between the reduced and oxidized forms of the active site peptide, has never been detected for PTP1b and may not be stable to trypsin and/or MALDI-MS conditions.

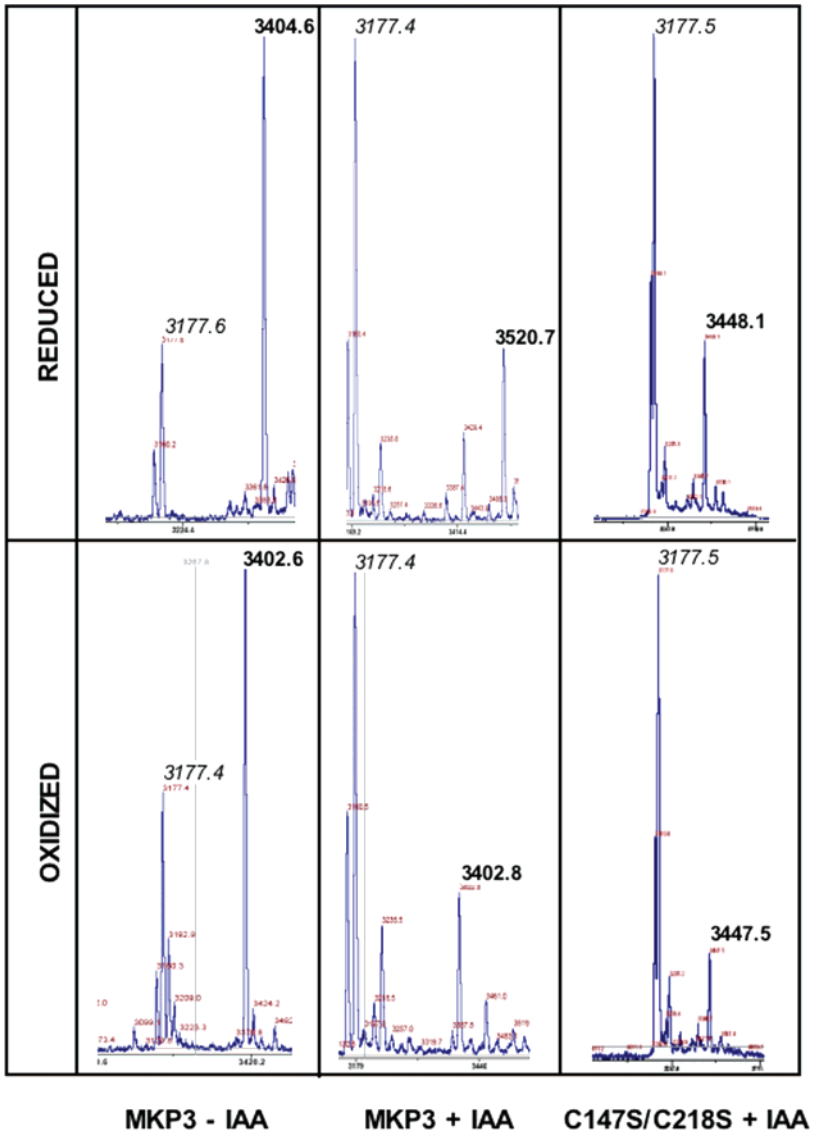

FIGURE 9: MALDI-MS mass spectra of reduced and oxidized MKP3. The region of the MALDI-MS spectrum containing the tryptic peptide containing Cys147 and Cys155 is shown for MKP3, MKP3 treated with IAA, and C147S/C218S treated with IAA, from left to right, respectively. The data for samples from reduced and oxidized protein are shown in the top and bottom rows, respectively. The Cys147-containing peptide is labeled in bold type, and other significant peptides are labeled in italic type. The reduced sample of MKP3 treated with IAA shows the modification of two cysteines compared to the untreated sample. The oxidized samples of MKP3 and MKP3 treated with IAA show a loss of 2 Da compared to the reduced protein, consistent with formation of an intrapeptide disulfide. The C147S/C218S mutant shows only one modified cysteine in both the reduced and oxidized samples.

To test possible formation of a sulfenyl−amide bond as a reaction intermediate upon oxidation for MKP3, Leu294 was mutated to proline. The sulfur atom of Cys293 in the L294P mutant should be unable to form a sulfenyl−amide bond, as the backbone nitrogen of the proline residue is already part of the proline ring. L294P had no detectable phosphatase activity, and hence, its inactivation by H_2O_2 or reactivation by DTT could not be characterized. Despite the absence of catalytic activity, however, the mass of the active site tryptic peptide from the oxidized protein was 2 Da lower than the mass from the reduced protein (1424 and 1426 Da, respectively; data not shown). The tryptic peptide containing Cys147/Cys155 is also found with a mass reduced by 2 Da following oxidation by H_2O_2 (3402 and 3404 Da, respectively; data not shown). No higher oxidation states such as the sulfenic acid were seen for the active site peptide. We conclude that the catalytic cysteine in the L294P mutant must still exist in a special environment where it can be readily oxidized. Additionally, as for the wild-type enzyme, the active site cysteine is protected from further oxidation by disulfide formation that can be detected as intrapeptide disulfides. These disulfides can form without a sulfenyl−amide intermediate.

DISCUSSION

One hundred PTPs exist in the human genome (*3*), all presumably with a highly reactive cysteine residue at the active site that needs to be protected from irreversible oxidation. For some PTPs, oxidation/reduction may serve as a regulatory mechanism, whereas for others, protection against irreversible oxidation may merely be a mechanism for maintaining the integrity of the enzyme against spurious oxidation. Whatever the reason, it is interesting to note the ever-increasing variety of mechanisms by which this protec-

tion against irreversible oxidation is ensured. For most PTPs that have been examined (e.g., low-molecular mass phosphatases, PTEN, KAP, and Cdc25), a disulfide is formed with a nearby backdoor cysteine following initial oxidation and sulfenic acid formation (*10*, *12*−*14*). For PTP1b, glutathionylation (*31*) or formation of a sulfenyl−amide bond (*16*, *17*) serves as the protective mechanism. An intermolecular disulfide bond is formed upon oxidation of the receptor PTP (*15*). In soybean *Glycine max* PTP, two cysteine residues near the catalytic cysteine, but not the catalytic cysteine, participate in redox regulation following S-glutathionylation (*32*). Herein, we expand the possible mechanisms of protection for PTPs as we find that MKP3 can use multiple cysteines in a distal domain to protect its active site from excessive oxidation. Not only does MKP3 have a functional backdoor cysteine in the proximity of the active site, like Cdc25, PTEN, and the low-molecular mass PTPs, but in the absence of this cysteine, it can utilize one of a number of cysteines residing in a different domain (including at least Cys147). Most amazing is the effectiveness at which these different cysteines can be utilized. Despite their somewhat diverse locations in the N-terminal domain (Figure 1), our data indicate that more than one of these cysteines is capable of rapidly reacting with the active site cysteine upon its initial oxidation to the sulfenic acid. Recall that in the absence of any protective cysteines (i.e., ΔC218S), the second oxidative step to the irreversibly oxidized sulfinic acid occurs >15-fold faster than the primary oxidative step (Figure 5). Although one might envision that the N-terminal domain simply excludes H_2O_2 to ensure protection against oxidation, this seems unlikely given the highly diffusive nature and small size of H_2O_2. The involvement of multiple N-terminal cysteines, whose complete dissection is beyond the scope of this work, is consistent with the following. First, formation of high-molecular mass oligomers has previously been observed following oxidation of the C39S, C127S, and C147S but not other cysteine mutants (*5*). We have observed similar high-molecular mass bands indicative of intermolecular disulfide formation for the C39S/C218S, C127S/C218S, and C147S/C218S mutants when one of the more optimal mechanisms is nonfunctional (Figure 8). However, oligomerization clearly is not the preferred pathway for any of these mutants, as indicated by the low intensity of these higher-molecular mass bands. Thus, intermolecular disulfide bond formation is most likely a secondary side reaction. These data further confirm that there is not just one cysteine in the N-terminal domain that can react with the active site sulfenic acid, instead suggesting that at least two of these cysteines can serve as a functional trap of the sulfenic acid. Second, the involvement of multiple cysteines in the N-terminus also further explains why we could not identify these cysteine residues from comparison of the MALDI- or ESI-MS spectra in peptidic fragments of reduced and oxidized MKP3. At any given time following oxidation, a nonhomogeneous population of MKP3 molecules that contain different pairs of cysteines in disulfide bonds apparently exists. These presumably can be interchanged by rapid disulfide exchange, and even when this process is quenched by addition of an alkylation agent (e.g., IAA), a mixed population of species becomes hard to identify on the basis of the low abundance. Thus, our result showing that more than one of the N-terminal cysteines serves as a highly efficient trap of the sulfenic acid expands the role for the N-terminal domain of MKP3, which had so far been known to play a role only in substrate binding. Also, the conserved Cys147 is essential for complete reactivation of oxidized MKP3 by thioredoxin.

In all previously studied PTPs that form an intramolecular disulfide bond upon oxidation, there has always been only one backdoor cysteine, present within the catalytic domain. This is the first example of a phosphatase in which cysteine residues present in a distal domain are involved in this process. As noted in the Results, we speculate Cys147 and potentially other N-terminal cysteines play the most important role in preventing the irreversible oxidation of MKP3. Why is the mechanism of redox control so much more complex for MKP3 than for other members of the PTP family? We suggest the mechanism of re-reduction requires the shuttling of the disulfide from the active site to a surface region more accessible to thioredoxin. We base this hypothesis on the multiple redox active cysteines that have been reported in the *Staphylococcus aureus* protein arsenate reductase (ArsC). ArsC is structurally similar to LMW-PTP and catalyzes the reduction of arsenate to arsenite (*33*). Upon arsenate reduction, the disulfide formed between the catalytic cysteine and the backdoor cysteine is buried and is inaccessible to thioredoxin (*34*). A disulfide switch with a second cysteine pair brings the disulfide bond to the surface, thus making it accessible for reduction by thioredoxin. For MKP3, we hypothesize that in a similar manner disulfide switches involving multiple cysteines in MKP3 could bring the buried disulfide formed between Cys293 and the original backdoor cysteine (Cys218) to the surface. The second cysteine pair in the disulfide switch could be conserved residues Cys39 and Cys147, with Cys147 forming the disulfide with thioredoxin. How these other cysteines can be so effective at replacing the backdoor cysteine in trapping of the primary sulfenic acid remains to be investigated further.

Our data showing the involvement of N-terminal cysteines in the protective mechanism against oxidation in MKP3 also suggest a possible orientation between these two domains. Recall that the structures of the N-terminal and C-terminal domains were determined separately by NMR and X-ray crystallography, respectively. Also, in the determination of the structure by NMR, the authors collected chemical shift perturbation data in the presence of the catalytic domain of the related phosphatase, PAC1, to suggest a possible orientation between the two domains. Although the binding between these two domains was weak (~100 μM), these results implicated the widely separated residues of α-helix 3 and α-helix 5, as well as some intervening loop residues (Figure 1). Cys39 and Cys147 are located between these two helices on a single side of the N-terminal domain that is compatible with these prior findings. We have not attempted to study the formation of disulfides between the two separate domains due to the reported weak interaction between them. However, we suggest that the conformation needed by MKP3 to accommodate disulfide bond formation of either of these two cysteines with the active site would block substrate access to the active site even more dramatically than we have recently observed for the disulfide form of Cdc25B (*25*). The two residues (Arg64 and Arg65) identified as the "hot spots" for interaction with ERK2 (*35*) lie on the same face of the MKP3 substrate binding domain as Cys39. Hence,

formation of a disulfide bond involving Cys39 could impair substrate binding. Conversely, ERK2 bound to MKP3 may prevent oxidative inactivation of MKP3.

In summary, our work identifies important elements of the complex pathway employed by MKP3 in preventing irreversible inactivation by oxidation. It has various unique features when compared to the strategies used by other PTPs. In general, PTPs that form disulfide bonds upon oxidation contain only one cysteine residue, designated as the backdoor cysteine that protects the active site. On the basis of the difference in reversibility of the C218S and ΔC218S mutants, we show that MKP3 can be rescued from irreversible oxidation by alternate pathways, at least one of which involves Cys147. We hypothesize that in the case of this phosphatase, disulfide switches can bring the buried primary disulfide bond to the surface of the protein to facilitate reduction by thioredoxin, a possibly common feature for these types of reductive mechanisms. The additional protective mechanisms seem appropriate for MKP3, a crucial component of the MAPK signaling pathway, and should caution one in making conclusions from studying these regulatory processes for other phosphatases using the catalytic domain alone.

ACKNOWLEDGMENT

We thank Ziqiang Guan in the group of Christian Raetz for his assistance with the MS/MS experiment, JoAnne Stubbe for the generous gift of TR/TRR, and John Denu for the expression plasmid for MKP3.

REFERENCES

1. Droge, W. (2002) Free radicals in the physiological control of cell function, *Physiol. Rev. 82*, 47−95.
2. Tonks, N. K. (2005) Redox redux: Revisiting PTPs and the control of cell signaling, *Cell 121*, 667−670.
3. Alonso, A., Sasin, J., Bottini, N., Friedberg, I., Friedberg, I., Osterman, A., Godzik, A., Hunter, T., Dixon, J., and Mustelin, T. (2004) Protein tyrosine phosphatases in the human genome, *Cell 117*, 699−711.
4. Kim, H. S., Song, M. C., Kwak, I. H., Park, T. J., and Lim, I. K. (2003) Constitutive induction of p-Erk1/2 accompanied by reduced activities of protein phosphatases 1 and 2A and MKP3 due to reactive oxygen species during cellular senescence, *J. Biol. Chem. 278*, 37497−37510.
5. Kamata, H., Honda, S.-I., Maeda, S., Chang, L., Hirata, H., and Karin, M. (2005) Reactive oxygen species promote TNFα-induced death and sustained JNK activation by inhibiting MAP kinase phosphatases, *Cell 120*, 649−661.
6. Stuckey, J. A., Schubert, H. L., Fauman, E. B., Zhang, Z.-Y., Dixon, J. E., and Saper, M. A. (1994) Crystal structure of *Yersinia* protein tyrosine phosphatase at 2.5 Å and the complex with tungstate, *Nature 370*, 571−575.
7. Peters, G. H., Frimurer, T. M., and Olsen, O. H. (1998) Electrostatic evaluation of the signature motif (H/V)CX5R(S/T) in protein-tyrosine phosphatases, *Biochemistry 37*, 5383−5393.
8. Denu, J. M., and Tanner, K. G. (1998) Specific and reversible inactivation of protein tyrosine phosphatases by hydrogen peroxide: Evidence for a sulfenic acid intermediate and implication for redox regulation, *Biochemistry 37*, 5633−5642.
9. Woo, E. S., Rice, R. L., and Lazo, J. S. (1999) Cell cycle dependent subcellular distribution of Cdc25B subtypes, *Oncogene 18*, 2770−2776.
10. Caselli, A., Marzocchini, R., Camici, G., Manao, G., Moneti, G., Pieraccini, G., and Ramponi, G. (1998) The inactivation mechanism of low molecular weight phosphotyrosine-protein phosphatase by H_2O_2, *J. Biol. Chem. 273*, 32554−32560.
11. Savitsky, P. A., and Finkel, T. (2002) Redox regulation of Cdc25C, *J. Biol. Chem. 277*, 20535−20540.
12. Sohn, J., and Rudolph, J. (2003) Catalytic and chemical competence of regulation of Cdc25 phosphatase by oxidation/reduction, *Biochemistry 42*, 10060−10070.
13. Lee, S.-R., Yang, K.-S., Kwon, J., Lee, C., Jeong, W., and Rhee, S. G. (2002) Reversible inactivation of the tumor suppressor PTEN by H_2O_2, *J. Biol. Chem. 277*, 20336−20342.
14. Song, H., Hanlon, N., Brown, N. R., Noble, M. E. M., Johnson, L. N., and Barford, D. (2001) Phosphoprotein−protein interactions revealed by the crystal structure of kinase-associated phosphatase in complex with phospho-Cdk2, *Mol. Cell 7*, 615−626.
15. van der Wijk, T., Overvoorde, J., and den Hertog, J. (2004) H_2O_2-induced intermolecular disulfide bond formation between receptor protein-tyrosine phosphatases, *J. Biol. Chem. 279*, 44355−44361.
16. van Montfort, R. L. M., Congreve, M., Tisi, D., Carr, R., and Jhoti, H. (2003) Oxidation state of the active site cysteine in protein tyrosine phosphatase 1B, *Nature 423*, 773−777.
17. Salmeen, A., Andersen, J. N., Myers, M. P., Meng, T.-C., Hinks, J. A., Tonks, N. K., and Barford, D. (2003) Redox regulation of protein tyrosine phosphatase 1B involves a sulphenyl-amide intermediate, *Nature 423*, 769−773.
18. Stewart, A. E., Dowd, S., Keyse, S., and McDonald, N. Q. (1999) Crystal structure of the MAPK phosphatase Pyst1 catalytic domain and implications for regulated activation, *Nat. Struct. Biol. 6*, 174−181.
19. Farooq, A., Chaturvedi, G., Mujtaba, S., Plotnikova, O., Zeng, L., Dhalluin, C., Ashton, R., and Zhou, M. M. (2001) Solution structure of ERK2 binding domain of MAPK phosphatase MKP-3: Structural insights into MKP-3 activation by ERK2, *Mol. Cell 7*, 387−399.
20. Wiland, A. M., Denu, J. M., Mourey, R. J., and Dixon, J. E. (1996) Purification and kinetic characterization of the mitogen-activated protein kinase phosphatase rVH6, *J. Biol. Chem. 271*, 33486−33492.
21. Camps, M., Nichols, A., Gillieron, C., Antonsson, B., Muda, M., Chabert, C., Boschert, U., and Arkinstall, S. (1998) Catalytic activation of the phosphatase MKP-3 by ERK2 mitogen-activated protein kinase, *Science 280*, 1262−1265.
22. Fjeld, C. C., Rice, A. E., Kim, Y., Gee, K., and Denu, J. M. (2000) Mechanistic basis for catalytic activation of mitogen-activated protein kinase phosphatase 3 by extracellular signal-regulated kinase, *J. Biol. Chem. 275*, 6749−6757.
23. Zhou, B., Wu, L., Shen, K., Zhang, J., Lawrence, D. S., and Zhang, Z. Y. (2001) Multiple regions of MAP kinase phosphatase 3 are involved in its recognition and activation by ERK2, *J. Biol. Chem. 276*, 6506−6515.
24. Keyse, S. M., and Ginsburg, M. (1993) Amino acid sequence similarity between CL100, a dual-specificity MAP kinase phosphatase and cdc25, *Trends Biochem. Sci. 18*, 377−378.
25. Buhrman, G., Parker, B., Sohn, J., Rudolph, J., and Mattos, C. (2005) Structural mechanism of oxidative regulation of the phosphatase Cdc25B via an intramolecular disulfide bond, *Biochemistry 44*, 5307−5316.
26. Winterbourn, C. C., and Metodiewa, D. (1999) Reactivity of biologically important thiol compounds with superoxide and hydrogen peroxide, *Free Radical Biol. Med. 27*, 322−328.
27. Goldman, R., Stoyanovsky, D. A., Day, B. W., and Kagan, V. E. (1995) Reduction of phenoxyl radicals by thioredoxin results in selective oxidation of its SH-groups to disulfides. An antioxidant function of thioredoxin, *Biochemistry 34*, 4765−4772.
28. Reynolds, R. A., Yem, A. W., Wolfe, C. L., Deibel, M. R. J., Chidester, C. G., and Watenpaugh, K. D. (1999) Crystal structure of the catalytic subunit of Cdc25B required for G2/M phase transition of the cell cycle, *J. Mol. Biol. 293*, 559−568.
29. Lee, J.-O., Yang, H., Georgescu, M.-M., Di Cristofano, A., Maehama, T., Shi, Y., Dixon, J. E., Pandolfi, P., and Pavletich, N. P. (1999) Crystal structure of the PTEN tumor suppressor: Implications for its phosphoinositide phosphatase activity and membrane association, *Cell 99*, 323−334.
30. Sivaramakrishnan, S., Keerthi, K., and Gates, K. S. (2005) A chemical model for redox regulation of protein tyrosine phosphatase 1B (PTP1B) activity, *J. Am. Chem. Soc. 127*, 10830−10831.
31. Barrett, W. C., DeGnore, J. P., König, S., Fales, H. M., Keng, Y.-F., Zhang, Z.-Y., Yim, M. B., and Chock, P. B. (1999)

Regulation of PTP1B via glutathionylation of the active site cysteine 215, *Biochemistry 38*, 6699−6705.

32. Dixon, D. P., Fordham-Skelton, A. P., and Edwards, R. (2005) Redox regulation of a soybean tyrosine-specific phosphatase, *Biochemistry 44*, 7679−7703.
33. Messens, J., Hayburn, G., Desmyter, A., Laus, G., and Wyns, L. (1999) The essential catalytic redox couple in arsenate reductase from *Staphylococcus aureus*, *Biochemistry 38*, 16857−16865.
34. Messens, J., Van Molle, I., Vanhaesebrouck, P., Limbourg, M., Van Belle, K., Wahni, K., Martins, J. C., Loris, R., and Wyns, L. (2004) How thioredoxin can reduce a buried disulphide bond, *J. Mol. Biol. 339*, 527−537.
35. Zhang, J., Zhou, B., Zheng, C.-F., and Zhang, Z.-Y. (2003) A bipartite mechanism for ERK2 recognition by its cognate regulators and substrates, *J. Biol. Chem. 278*, 29901−29912.

BI060157P